THE JOURNAL OF BIOLOGICAL CHEMISTRY VOL. 281, NO. 18, pp. 12300–12307, May 5, 2006

Corynebacterial Protein Kinase G Controls 2-Oxoglutarate Dehydrogenase Activity via the Phosphorylation Status of the OdhI Protein*[S]

Received for publication, November 22, 2005, and in revised form, March 1, 2006 Published, JBC Papers in Press, March 7, 2006, DOI 10.1074/jbc.M512515200

Axel Niebisch, Armin Kabus, Christian Schultz, Brita Weil, and Michael Bott[1]

From the Institut für Biotechnologie 1, Forschungszentrum Jülich, D-52425 Jülich, Germany

A novel regulatory mechanism for control of the ubiquitous 2-oxoglutarate dehydrogenase complex (ODH), a key enzyme of the tricarboxylic acid cycle, was discovered in the actinomycete *Corynebacterium glutamicum*, a close relative of important human pathogens like *Corynebacterium diphtheriae* and *Mycobacterium tuberculosis*. Based on the finding that a *C. glutamicum* mutant lacking serine/threonine protein kinase G (PknG) was impaired in glutamine utilization, proteome comparisons led to the identification of OdhI as a putative substrate of PknG. OdhI is a 15-kDa protein with a forkhead-associated domain and a homolog of mycobacterial GarA. By using purified proteins, PknG was shown to phosphorylate OdhI at threonine 14. The glutamine utilization defect of the Δ*pknG* mutant could be abolished by the additional deletion of *odhI*, whereas transformation of a Δ*odhI* mutant with a plasmid encoding OdhI-T14A caused a defect in glutamine utilization. Affinity purification of OdhI-T14A led to the specific copurification of OdhA, the E1 subunit of ODH. Because ODH is essential for glutamine utilization, we assumed that unphosphorylated OdhI inhibits ODH activity. In fact, OdhI was shown to strongly inhibit ODH activity with a K_i value of 2.4 nM. The regulatory mechanism described offers a molecular clue for the reduced ODH activity that is essential for the industrial production of 1.5 million tons/year of glutamate with *C. glutamicum*. Moreover, because this signaling cascade is likely to operate also in mycobacteria, our results suggest that the attenuated pathogenicity of mycobacteria lacking PknG might be caused by a disturbed tricarboxylic acid cycle.

Increasing numbers of eukaryotic-like serine/threonine protein kinases found in bacteria implicate that they play important roles in cell signaling, but their targets and specific functions are largely unknown (1). The genome of the important human pathogen *Mycobacterium tuberculosis* encodes 11 members of this protein family (2). Among these, protein kinase G (PknG)[2] gained particular interest because it was reported to inhibit phagosome-lysosome fusion, thus allowing for intracellular survival of mycobacteria. Deletion of the *pknG* gene in *Mycobacterium bovis* BCG resulted in lysosomal localization and mycobacterial cell death in infected macrophages. PknG was detected in the cytosol of infected macrophages and was therefore suggested to interfere with host cell signaling pathways (3). A *pknG* deletion mutant of *M. tuberculosis* displayed decreased viability upon infection of immunocompetent mice but also reduced growth *in vitro* (4), implying that PknG function is not restricted to the pathogenic life style. This is supported by the fact that genes encoding PknG homologs are not only present in pathogenic mycobacteria but also in all other members of the suborder Corynebacterineae with known genome sequence, *i.e.* species of the genera *Corynebacterium*, *Mycobacterium*, *Nocardia*, and *Rhodococcus*, as well as in *Streptomyces* species. To determine the function of PknG, we chose *Corynebacterium glutamicum*, a nonpathogenic species used for biotechnological amino acid production (5), which already proved useful for understanding the function of homologous genes in *M. tuberculosis* (6).

EXPERIMENTAL PROCEDURES

Bacterial Strains and Culture Conditions—The strains and plasmids used in this study are listed in Table 1. *C. glutamicum* strains were cultivated aerobically in shake flasks at 150 rpm and 30 °C in brain heart infusion medium (Difco) or CGXII minimal medium (7) with 200 mM glucose. For growth experiments on glutamine as carbon and nitrogen source, *C. glutamicum* was precultured overnight in brain heart infusion medium with 100 mM glucose. Cells were harvested, washed with 0.9% NaCl, and used to inoculate the main cultures in glutamine medium (modified CGXII lacking ammonium sulfate and urea and containing 100 mM glutamine) supplemented with 5 mM glucose. Samples for determination of intracellular metabolites and for proteome analysis were taken after 12 h of cultivation when the Δ*pknG* strain just became stationary after glucose depletion. For the determination of growth rates, cells grown in brain heart infusion medium with glucose were cultivated in glutamine medium with 20 mM glucose. The cells from this second preculture were used to inoculate glutamine medium without glucose. For all cloning purposes, *Escherichia coli* DH5α was used and routinely grown in Luria-Bertani medium at 37 °C. When appropriate, kanamycin was added at concentrations of 25 mg/liter (*C. glutamicum*) or 50 mg/liter (*E. coli*).

Construction of Plasmids and Mutants—The oligonucleotides used as PCR primer in this study are listed in Table S1. Plasmids were constructed by standard molecular genetic methods and confirmed by DNA sequence analysis. Defined *C. glutamicum* deletion mutants were constructed by crossover PCR and double homologous recombination using the suicide vector pK19mobsacB (8). All deletions were verified by Southern blot analysis. Site-directed mutagenesis of *odhI* was carried out by PCR using the mutagenic primer pairs T14A-for/-rev and T15A-for/-rev. For construction of *C. glutamicum* strains synthesizing Strep-tagged OdhA or Strep-tagged AceE, 3′-terminal fragments of the respective genes were amplified with the primer pairs *odhA*-for/*odhA*-rev and *aceE*-for/*aceE*-rev. The reverse primers introduced a Strep-

* This work was supported in part by Grant 0312843B from the German Ministry of Education and Research (to M. B.). The costs of publication of this article were defrayed in part by the payment of page charges. This article must therefore be hereby marked "*advertisement*" in accordance with 18 U.S.C. Section 1734 solely to indicate this fact.

[S] The on-line version of this article (available at http://www.jbc.org) contains Table S1.

[1] To whom correspondence should be addressed: Institut für Biotechnologie 1, Forschungszentrum Jülich, D-52425 Jülich, Germany. Tel.: 49-2461-615515; Fax: 49-2461-612710; E-mail: m.bott@fz-juelich.de.

[2] The abbreviations used are: PknG, protein kinase G; FHA, forkhead-associated; ODH, 2-oxoglutarate dehydrogenase; PDH, pyruvate dehydrogenase; TES, 2-{[2-hydroxy-1,1-bis(hydroxymethyl)ethyl]amino}ethanesulfonic acid.

TABLE 1
Plasmids and *C. glutamicum* strains used in this study

	Description	Ref.
Strains		
ATCC13032	Biotin-auxotrophic wild-type strain	39
Δ*pknG*	Wild type derivative with in-frame deletion of *pknG* (*cg3046*)	This work
Δ*glnH*	Wild type derivative with in-frame deletion of *glnH* (*cg3045*)	This work
Δ*glnX*	Wild type derivative with in-frame deletion of *glnX* (*cg3044*)	This work
Δ*odhI*	Wild type derivative with in-frame deletion of *odhI* (*cg1630*)	This work
Δ*pknG*Δ*odhI*	Δ*pknG* derivative with additional in-frame deletion of *odhI*	This work
WT-$odhA_{St}$	Wild type derivative with plasmid pK18mob-$odhA_{St}$ integrated into the chromosomal *odhA* gene (*cg1280*) adding a Strep-tag-II coding sequence before the *odhA* stop codon	This work
Δ*pknG*-$odhA_{St}$	As above but Δ*pknG* derivative	This work
WT-$aceE_{St}$	Wild type derivative with plasmid pK18mob-$aceE_{St}$ integrated into the chromosomal *aceE* gene (*cg2466*) adding a Strep-tag-II coding sequence before the *aceE* stop codon	This work
Δ*pknG*-$aceE_{St}$	As above but Δ*pknG* derivative	This work
Plasmids		
pEKEx2	Kan^R, *C. glutamicum* expression vector for IPTG-inducible gene expression	40
pEKEx2-$pknG_{St}$	pEKEx2 derivative containing the *C. glutamicum pknG* gene with the native ribosome-binding site and a Strep-tag-II coding sequence before the *pknG* stop codon	This work
pAN3K	Kan^R, derivative of the *E. coli* expression vector pASK-IBA3C (IBA, Göttingen, Germany) for anhydrotetracycline-inducible production of C-terminally Strep-tagged proteins, contains the Kan^R gene and the *C. glutamicum* replicon from pJC1 allowing plasmid replication and gene expression in *C. glutamicum*	This work
pAN3K-*odhI* and derivatives	pAN3K derivative containing the *C. glutamicum* wild-type *odhI* gene (obtained by PCR with primers *OdhI*-for-1/rev-1) or mutated *odhI* genes with Thr-14 or -15 codons exchanged to alanine codons	This work
pJC1	Kan^R, *E. coli-C. glutamicum* shuttle vector	41
pJC1-*odhI* and derivatives (T14A, T15A)	pJC1 derivatives containing the *C. glutamicum* wild-type *odhI* gene (obtained by PCR with primers *OdhI*-for-2/-rev-2) with its native promoter or mutated *odhI* genes with Thr-14 or -15 codons exchanged to alanine codons; a Strep-tag-II coding sequence before the *odhI* stop codon was introduced by the reverse primer	This work
pK18mob	Kan^R, *E. coli* vector unable to replicate in *C. glutamicum*	42
pK18m-$odhA_{St}$	pK18mob derivative containing a 625-bp PCR product covering the 3′-terminal end of the *odhA* gene elongated with a Strep-tag-II coding sequence before the stop codon	This work
pK18m-$aceE_{St}$	pK18mob derivative containing a 578-bp PCR product covering the 3′-terminal end of the *aceE* gene elongated with a Strep-tag-II coding sequence before the stop codon	This work
pK19mobsacB	Kan^R, *E. coli* vector for generating *C. glutamicum* deletion mutants	42
pK19ms-Δ*pknG*	pK19mobsacB derivative containing a crossover PCR product (primer Δ*pknG*-1–4) that covers the flanking regions of the *pknG* gene	This work
pK19ms-Δ*glnH*	pK19mobsacB derivative containing a crossover PCR product (primer Δ*glnH*-1–4) that covers the flanking regions of the *glnH* gene	This work
pK19ms-Δ*glnX*	pK19mobsacB derivative containing a crossover PCR product (primer Δ*glnX*-1–4) that covers the flanking regions of the *glnX* gene	This work
pK19ms-Δ*odhI*	pK19mobsacB derivative containing a crossover PCR product (primer Δ*odhI*-1–4) that covers the flanking regions of the *odhI* gene	This work

tag-II coding sequence before the stop codon. After cloning the PCR products into the suicide vector pK18mob, the resulting plasmids were integrated into the *C. glutamicum* chromosome by a single homologous recombination event. Recombinant strains were selected on agar plates containing kanamycin.

Determination of Internal Glutamine/Glutamate Concentrations—Culture samples containing 0.5–1 mg of biomass (dry weight) were rapidly filtered through glass fiber disks (Millipore), and the filter-bound cells were washed with 0.9% NaCl at room temperature (9). Internal metabolites were extracted by incubating harvested cells in 1.3 ml of 50 μM ornithine for 15 min at 95 °C. Amino acids in the extracts were quantified by high pressure liquid chromatography after precolumn derivatization with *o*-phthaldialdehyde. Internal concentrations were calculated using a correlation of dry weight (mg/ml) = $0.25 \times A_{600}$ and a cytoplasmic volume of 1.5 μl/mg dry weight (10). The correlation between dry weight and OD_{600} was determined for three independent cultures of wild type and Δ*pknG* mutant and was found to be identical.

Two-dimensional Gel Electrophoresis and Protein Identification—Cytosolic proteins were isolated and separated by two-dimensional gel electrophoresis as described (11). Protein identification from Coomassie-stained one- or two-dimensional gels and analysis of the OdhI phosphorylation site was performed by peptide mass fingerprinting of tryptic digests and post-source decay analysis of the phosphorylated peptide using a Voyager DE-STR mass spectrometer (Applied Biosystems, Weiterstadt, Germany) as described (11).

Preparation of Cell-free Extracts and Protein Purification by Affinity Chromatography—All steps were performed at 4 °C. Generally, cells were resuspended in buffer A (100 mM Tris/HCl, pH 8.0, 150 mM NaCl) containing Complete EDTA-free protease inhibitor (Roche Diagnostics) and disrupted by sonication or French press treatment. Cell debris was removed by low speed centrifugation (18,000 × *g* for 10 min). Prior to purification, cell extracts from *C. glutamicum* were incubated with avidin (50 μg/mg protein) for 30 min to reduce copurification of the biotinylated proteins pyruvate carboxylase and acyl-CoA carboxylase. Strep-tagged PknG, OdhI, and mutated derivatives were purified from *C. glutamicum* Δ*pknG*/pEKEx2-$pknG_{St}$ and *E. coli* DH5α containing pAN3K-*odhI*, pAN3K-*odhI*-T14A, or pAN3K-*odhI*-T15A, respectively, by affinity chromatography on *Strep*-Tactin-Sepharose columns (1-ml bed volume, IBA, Göttingen, Germany). Cell extracts (≤5 mg of protein/ml) were applied to the column and washed with 6 ml of buffer A, and bound proteins were eluted in 3 ml of buffer A with 2.5 mM desthiobiotin. Fractions containing the purified proteins were concentrated by ultrafiltration and stored frozen at −20 °C in elution buffer containing 20% (v/v) glycerol. For copurification attempts of OdhI and OdhA on analytical scale, *Strep*-Tactin-coated magnetic beads (IBA, Göttingen) were used. 10 mg of beads were activated according to the supplier's instructions, equilibrated in buffer A, and mixed with 2 ml of cell extract. After 1 h of incubation with occasional shaking, the beads were separated and washed five times with 200 μl of buffer A, and bound proteins were eluted in 100 μl of buffer A with 2.5 mM desthiobiotin.

For 2-oxoglutarate dehydrogenase (ODH) and pyruvate dehydrogenase (PDH) activity assays and for purification of active ODH·PDH complexes, cells were disrupted in buffer B (50 mM TES/NaOH, pH 7.7, 10 mM $MgCl_2$) with 30% (v/v) glycerol. Cell extracts for enzyme assays were gel-filtrated in the same buffer on PD10 columns (Amersham Biosciences) to remove interfering intracellular metabolites. ODH·PDH complexes were purified on *Strep*-Tactin-coated magnetic beads or *Strep*-Tactin-Sepharose (for subsequent enzyme assays) essentially as described above, but cell extracts were diluted with buffer B to 15% (v/v) glycerol, and buffer A was replaced by buffer B containing 10% (v/v) glycerol.

Enzyme Assays—Autokinase activity of PknG and PknG-dependent phosphorylation of OdhI was assayed in kinase buffer (25 mM Tris/HCl, pH 7.5, 5 mM $MgCl_2$, 2 mM $MnCl_2$, 1 mM dithiothreitol) as described (12). Oxoglutarate dehydrogenase and pyruvate dehydrogenase activity were measured at 30 °C in a photometric assay by following the initial increase in absorbance of NADH at 340 nm (13). Assays containing buffer B with 3 mM L-cysteine, 0.9 mM thiamine diphosphate, 2 mM NAD^+, 50 μM chlorpromazine (to prevent reoxidation of NADH (14)), 25–100 μl of cell extract, or purified ODH·PDH complexes and up to 30.4 nM OdhI were preincubated for 10 min at 30 °C before the reaction was started by addition of 1.5 mM 2-oxoglutarate or pyruvate and 0.2 mM coenzyme A. An activity of 1 unit refers to 1 μmol of NADH formed per min.

Miscellaneous—Protein concentrations were determined with the Bradford protein assay using bovine serum albumin as standard. Glutamine uptake rates of cells grown in CGXII/glucose to the mid-log phase were determined using 1-[^{14}C]glutamine and a filtration assay as described (15).

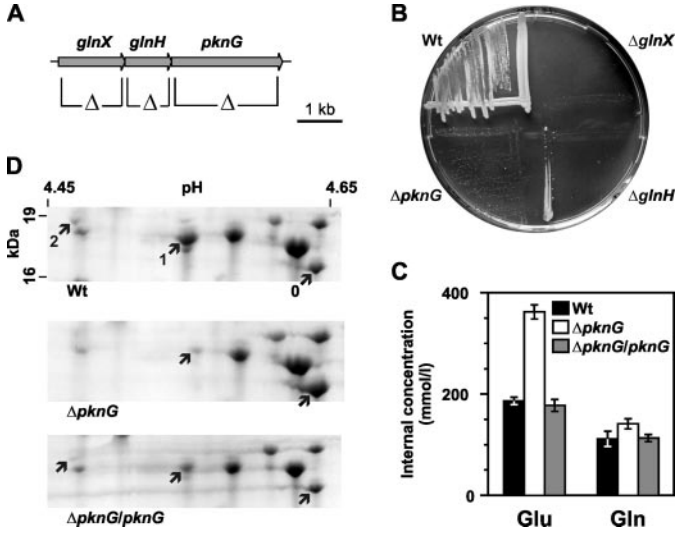

FIGURE 1. **Genomic organization of the *pknG* gene and consequences of its deletion in *C. glutamicum*.** *A*, the *pknG* gene for protein kinase G is clustered with *glnX* and *glnH* encoding an integral membrane protein of unknown function and a putative glutamine-binding lipoprotein, respectively. The chromosomal deletions present in strains Δ*pknG*, Δ*glnX*, and Δ*glnH* are indicated. *B*, growth of *C. glutamicum* wild type (*Wt*) and strains lacking *pknG*, *glnH*, or *glnX* on minimal medium agar with 100 mM glutamine as sole carbon source after 3 days at 30 °C. *C* and *D*, phenotypic characterization of *C. glutamicum* wild type, Δ*pknG* mutant, and complemented Δ*pknG* mutant during growth in minimal medium with 100 mM glutamine and 5 mM glucose. *C*, internal concentrations of glutamate and glutamine. The data represent mean values ± S.D. of three separate cultures. *D*, sections of representative two-dimensional gels showing three protein spots (indicated with *arrows*) with altered abundance in the Δ*pknG* mutant compared with wild type and complemented Δ*pknG* mutant. The spots correspond to the unphosphorylated (*spot 0*), monophosphorylated (*spot 1*) and putative doubly phosphorylated (*spot 2*) form of OdhI (encoded by *cg1630*).

RESULTS

PknG Is Required for Glutamine Utilization in C. glutamicum—The *C. glutamicum pknG* gene (*cg3046*) is located in a putative operon (Fig. 1*A*) with two genes, *cg3044* (*glnX*) and *cg3045* (*glnH*), that encode a hypothetical membrane protein with four potential transmembrane helices and a putative "periplasmic" glutamine-binding lipoprotein, respectively (16). This gene arrangement is conserved in bacteria containing *pknG* homologs except for *Streptomyces coelicolor* and *Streptomyces avermitilis* where an additional open reading frame is present between *glnH* and *pknG*. Because GlnH homologs of other bacteria, *e.g. E. coli* or *Bacillus subtilis*, are part of ABC transporters for high affinity glutamine uptake, we tested the effect of an in-frame *pknG* deletion in *C. glutamicum* on glutamine utilization. As shown in Fig. 1*B*, *C. glutamicum* wild type grew on minimal medium agar plates with glutamine as sole carbon and nitrogen source, whereas growth of the Δ*pknG* mutant was severely inhibited. This phenotype could be complemented by plasmid-borne *pknG* (data not shown). In liquid glutamine medium, *C. glutamicum* wild type showed a growth rate of 0.17–0.20 h^{-1} and formed 5 g of cell dry weight $liter^{-1}$ within 20 h. The Δ*pknG* strain showed no growth within this period. The mutant started to grow only after a prolonged incubation. This growth was probably because of suppressor mutations, because the lag phase of different cultures varied considerably, and cells from these cultures could subsequently grow immediately on glutamine agar plates. No significant growth differences were observed on rich medium or glucose minimal medium (data not shown). To study the role of GlnX and GlnH for glutamine utilization, in-frame deletion mutants of *C. glutamicum* lacking either *glnX* or *glnH* were constructed (Fig. 1*A*). On glutamine agar plates, both mutants showed a growth defect (Fig. 1*B*). In liquid glutamine medium, the Δ*glnX* mutant showed a similar phenotype as the Δ*pknG* mutant. There was no growth within 50 h, but upon prolonged incubation suppressor mutants started to grow. By contrast, the Δ*glnH* mutant was able to grow in liquid glutamine medium, with growth rates varying from 0.14 to 0.16 h^{-1}. From these results, a function of PknG, GlnX, and GlnH in glutamine uptake or metabolism could be inferred.

C. glutamicum possesses a secondary Na^+-dependent glutamine uptake system that has not yet been genetically identified (15). Transport assays were performed to study whether GlnH and GlnX are part of a glutamine transporter that is regulated by PknG. However, the *C. glutamicum* mutant strains lacking *pknG*, *glnX*, or *glnH* showed at least 80% of the glutamine transport activity of the wild type (data not shown), indicating that the defect of the mutants in glutamine utilization is not because of an impaired glutamine uptake. A similar result was reported for a *M. bovis* BCG Δ*pknG* mutant (17). Measurement of the internal amino acid concentrations revealed that the glutamate level was 2-fold higher in the Δ*pknG* mutant compared with the wild type and the complemented mutant, whereas the glutamine level was only slightly increased (Fig. 1*C*). Therefore, a defect in glutamate catabolism was likely to be responsible for the defect of the Δ*pknG* mutant in glutamine utilization.

Identification of an in Vivo Substrate of PknG—To find the molecular basis for inhibition of glutamate catabolism by PknG, we searched for *in vivo* phosphorylation substrates of PknG by proteome analysis of *C. glutamicum* wild type, Δ*pknG* mutant, and complemented mutant grown on 100 mM glutamine and 5 mM glucose as carbon sources. Comparison of Coomassie-stained two-dimensional gels revealed a series of three spots in the acidic, low molecular mass range that clearly differed between the wild type and complemented Δ*pknG* strain on the one hand and the Δ*pknG* mutant on the other hand (Fig. 1*D*). All three spots were identified by mass spectrometry as the protein encoded by gene *cg1630*, which was designated OdhI. OdhI (143 amino acid resi-

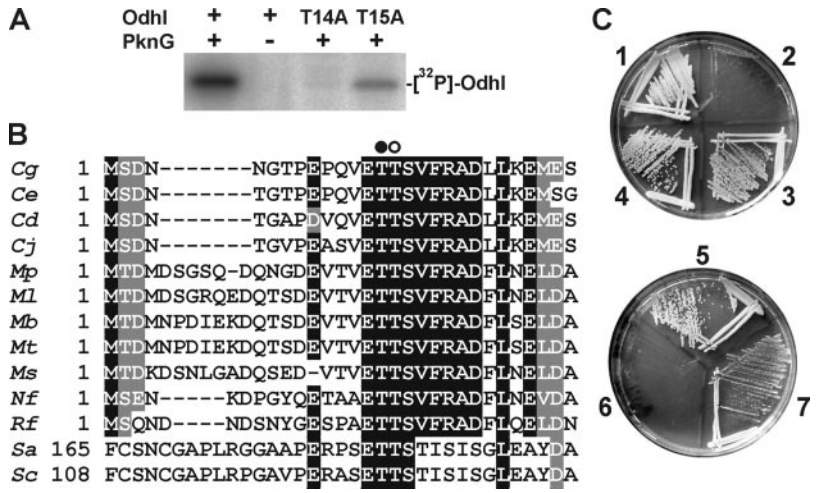

FIGURE 2. **Phosphorylation of OdhI by PknG and role of OdhI for glutamine utilization.** *A*, autoradiogram showing *in vitro* phosphorylation of OdhI by PknG at threonine 14. A T14A exchange in OdhI abolishes phosphorylation, whereas a T15A exchange does not. 61 pmol of OdhI or the indicated variants were incubated with 5.6 pmol of PknG and 37 kBq [γ-^{32}P]ATP for 30 min at 37 °C, denatured, and completely loaded on a 15% SDS gel. *B*, alignment of the amino-terminal regions of OdhI homologs from different *Actinomycetales*. The *filled circle* denotes the residue in *C. glutamicum* OdhI that is phosphorylated by PknG and the *open circle* the residue of the *M. tuberculosis* OdhI homolog (designated GarA), which is phosphorylated *in vitro* by PknB (20). *Ce*, *Corynebacterium efficiens*; *Cj*, *Corynebacterium jeikeium*; *Mp*, *Mycobacterium avium* subsp. *paratuberculosis*; *Mb*, *M. bovis*; *Mt*, *M. tuberculosis*; *Ms*, *M. smegmatis*; *Rf*, *Rhodococcus fascians*; *Sa*, *S. avermitilis*; *Sc*, *S. coelicolor*. *C*, growth with glutamine as sole carbon source of the following *C. glutamicum* strains: *1*, wild type; *2*, Δ*pknG*; *3*, Δ*odhI*; *4*, Δ*pknG*Δ*odhI*; *5*, Δ*odhI*/pJC1; *6*, Δ*odhI*/pJC1-*odhI*-T14A; *7*, Δ*odhI*/pJC1-*odhI*-T15A.

dues, 15,402 Da) is a homolog (69% sequence identity) of *Mycobacterium smegmatis* GarA (18) and contains a forkhead-associated (FHA) domain, which binds phosphothreonine epitopes on proteins and mediates phosphorylation-dependent protein-protein interactions (19). The pI values of 4.64, 4.56, and 4.47 observed for the three OdhI spots were close to the theoretical values calculated for unphosphorylated, monophosphorylated, and doubly phosphorylated OdhI protein, respectively. The amount of the different OdhI isoforms was relatively quantified by densitometric analysis of the two-dimensional gels. In the wild type 61.5 ± 6.4% of total OdhI was present in the monophosphorylated and 5.5 ± 3.9% in the doubly phosphorylated form (all data are mean values ± S.D. of three gels from independent cultures). The complemented Δ*pknG* mutant showed no significant differences with corresponding values of 53.1 ± 14.3 and 2.0 ± 1.8%, respectively. In contrast, the Δ*pknG* mutant contained only 5.9 ± 0.1% monophosphorylated OdhI, and the doubly phosphorylated form was undetectable. These data suggest that OdhI is phosphorylated by PknG but also by at least one additional protein kinase. Besides PknG, *C. glutamicum* possesses homologs of the *M. tuberculosis* serine/threonine protein kinases PknA, PknB, and PknL (2), encoded by the genes *cg0059*, *cg0057,* and *cg2388*, respectively. As *M. tuberculosis* PknB was recently shown to phosphorylate mycobacterial GarA *in vitro* (20), PknB is a favorite candidate for PknG-independent OdhI phosphorylation.

To confirm that OdhI is a substrate of PknG, both proteins were synthesized as Strep-tagged derivatives and purified to apparent homogeneity. As shown by *in vitro* kinase assays, PknG catalyzed autophosphorylation and transphosphorylation of OdhI, whereas OdhI alone did not incorporate ^{32}P (Fig. 2*A*). By comparing the tryptic peptide mass fingerprints of phosphorylated and unphosphorylated OdhI, the amino-terminal peptide covering amino acid residues 2–19 was found to be the only one phosphorylated by PknG (Fig. 3, *A* and *B*). Post-source decay analysis of this peptide identified threonine 14 as the phosphorylated residue (Fig. 3*C*). This result was verified by *in vitro* kinase assays, which showed that a T14A exchange in OdhI abolished PknG-dependent phosphorylation (Fig. 2*A*). In contrast, a T15A exchange only reduced the phosphorylation efficiency, indicating that Thr-15 might be involved in the binding of OdhI to PknG. OdhI/GarA homologous proteins with a strictly conserved ETTS motif in the amino-terminal region occur in all species that contain PknG homologs (Fig. 2*B*). The first threonine residue of this motif is the one phosphorylated by PknG in *C. glutamicum*, and the second threonine residue corresponds to Thr-22 of GarA from *M. tuberculosis* that was shown to be phosphorylated by PknB (20).

Functional Characterization of the PknG Substrate OdhI—To address the *in vivo* function of OdhI, in particular its involvement in glutamine utilization, its structural gene was deleted in *C. glutamicum* wild type as well as in the Δ*pknG* mutant. Additionally, the Δ*odhI* mutant was transformed with plasmids pJC1-*odhI*, pJC1-*odhI*-T14A, or pJC1-*odhI*-T15A directing the synthesis of Strep-tagged OdhI, OdhI-T14A, or OdhI-T15A, respectively. The Δ*odhI* mutant was able to grow on glutamine, and the defect of the Δ*pknG* mutant in glutamine utilization was abolished by additional deletion of *odhI* (Fig. 3*C*), showing that OdhI is an essential component of the PknG signaling pathway and pointing to an inhibitory function of unphosphorylated OdhI. Consistently, the Δ*odhI* strain synthesizing the OdhI-T14A protein could not grow on glutamine agar plates, whereas the one with the OdhI-T15A protein could (Fig. 3*C*). In summary, the presence of OdhI, which cannot be phosphorylated on Thr-14 by PknG, inhibited growth on glutamine and consequently glutamate degradation.

In contrast to proteins containing the FHA domain as part of a larger protein whose activity is modulated by phosphorylation (21, 22), the FHA domain of the OdhI protein is flanked only by an amino-terminal extension of about 50 amino acid residues. This suggested that OdhI exerts its inhibitory function in glutamate catabolism by interaction with other cellular proteins. To identify OdhI interaction partners, plasmid-encoded Strep-tagged OdhI-T14A was purified from *C. glutamicum* strain Δ*odhI*. As shown in Fig. 4*A*, large amounts of a protein with an apparent mass of 140 kDa were copurified, which was identified by mass spectrometry as OdhA (*cg1280*), the E1o subunit of the 2-oxoglutarate dehydrogenase complex (23). In contrast, only small amounts of OdhA were copurified with unmutated OdhI from strain Δ*odhI*/pJC1-*odhI*, which was present predominantly in the phosphorylated form, suggesting that OdhA interacts preferably with unphosphorylated OdhI (Fig. 4*A*, *lane 2*). This was further strengthened by copurification of unphosphorylated OdhI with Strep-tagged OdhA (Fig. 4*A*, *lane 3*). The phenotype of the *odhI* mutants along with the observation that

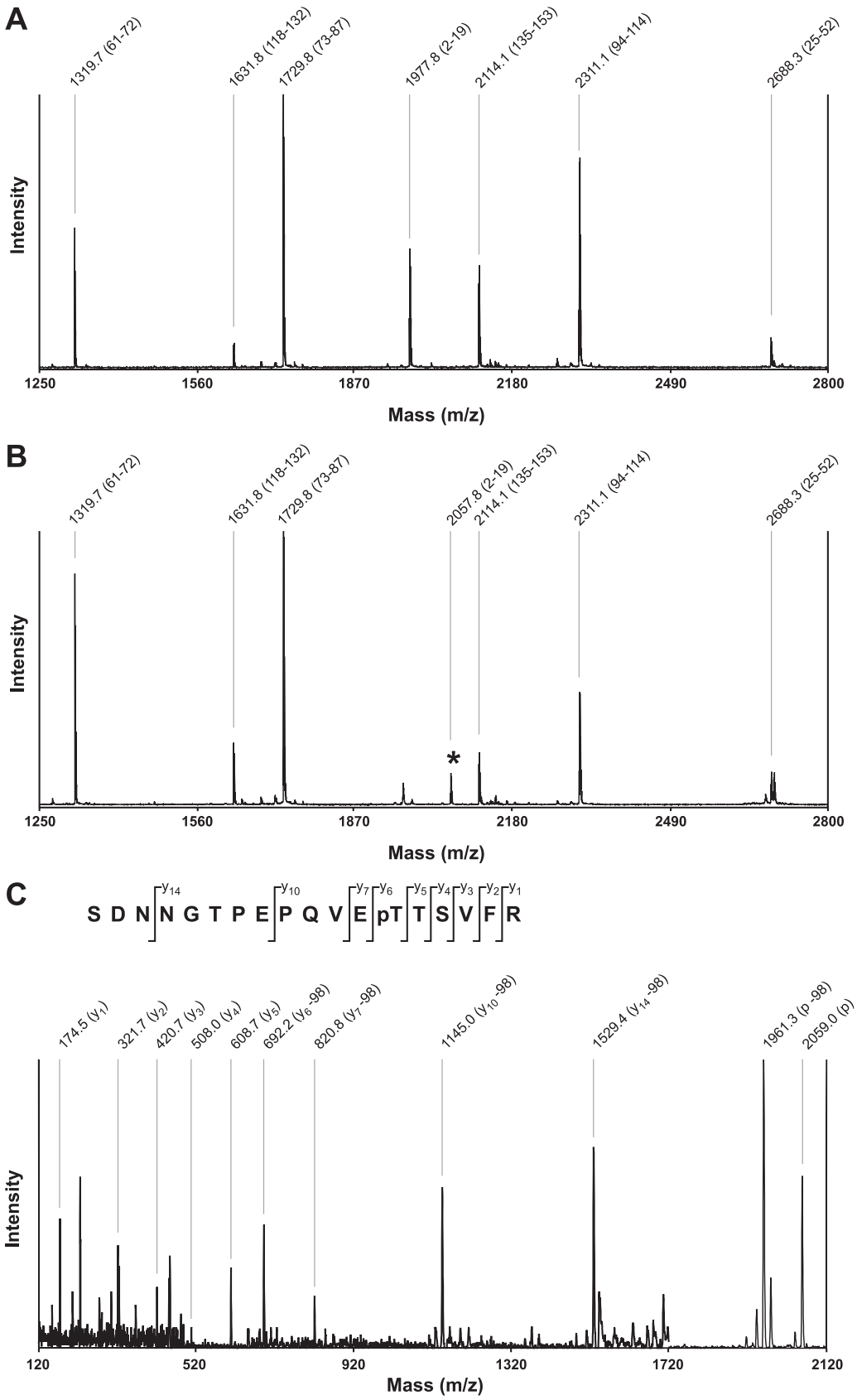

FIGURE 3. **Mapping of the PknG-dependent phosphorylation site of OdhI.** Peptide mass fingerprints of tryptic digests of unphosphorylated (*A*) and *in vitro* phosphorylated (*B*) Strep-tagged OdhI. Peaks are labeled with their monoisotopic masses and the assigned amino acid residues are shown in *parentheses*. The covered sequence (87% of 153 amino acids) included all serine and threonine residues. The putative phosphopeptide is marked with an *asterisk*. *C*, post-source decay analysis of the OdhI phosphopeptide (average mass 2059.0). For noise filtering and smoothing, the Data Explorer software (Applied Biosystems) was used. Fragment ions attributable to the *y*-series within a mass accuracy of 0.7 Da were labeled. β-Elimination of phosphoric acid (mass shift −98) is indicated.

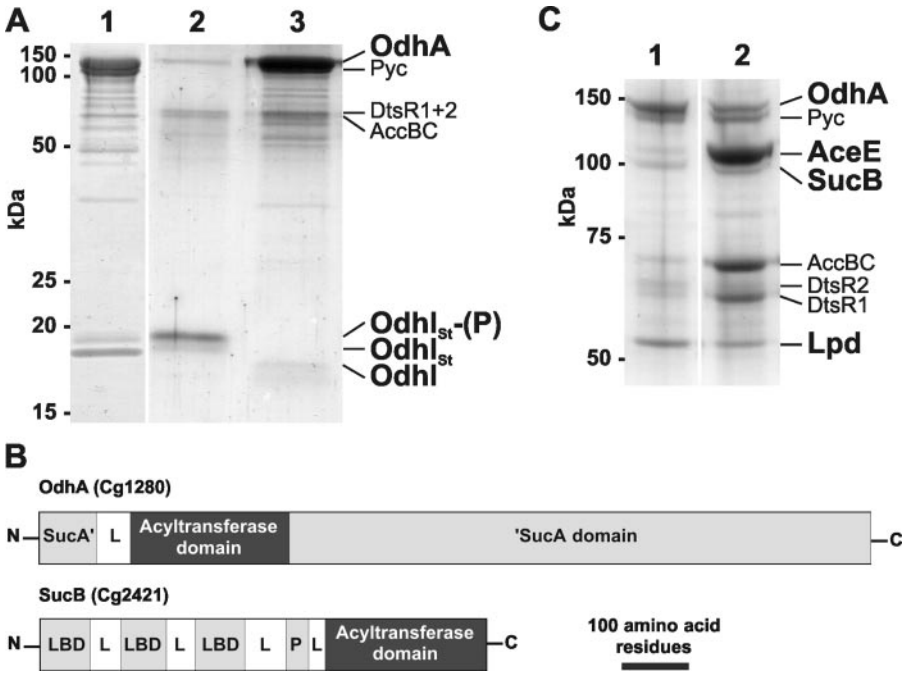

FIGURE 4. **Interaction of unphosphorylated OdhI with the E1 subunit (OdhA) of ODH and evidence for a mixed 2-oxoglutarate-pyruvate dehydrogenase complex.** *A*, copurification of native OdhA with Strep-tagged OdhI-T14A from *C. glutamicum* Δ*odhI*/pJC1-*odhI*-T14A (*lane 1*) or with Strep-tagged OdhI from *C. glutamicum* Δ*odhI*/pJC1-*odhI* (*lane 2*) and copurification of native OdhI with Strep-tagged OdhA from *C. glutamicum* WT-$odhA_{St}$ (*lane 3*). Note that pyruvate carboxylase (*Pyc*) and acyl-CoA carboxylase (AccBC, DtsR1, DtsR2) were copurified because of direct binding of their biotin prosthetic groups to the *Strep*-Tactin-Sepharose matrix. *B*, domain organization of the E1 (OdhA) and E2 (SucB) subunits of ODH of *C. glutamicum*. *L*, linker; *LBD*, lipoyl binding domain; *P*, peripheral subunit binding domain. *C*, purification of a mixed 2-oxoglutarate-pyruvate dehydrogenase complex consisting of the E1 subunits of ODH (OdhA), PDH (AceE), E2 (SucB), and E3 (Lpd) either via Strep-tagged OdhA from *C. glutamicum* WT-$odhA_{St}$ (*lane 1*) or via Strep-tagged AceE from *C. glutamicum* WT-$aceE_{St}$ (*lane 2*).

ODH activity is crucial for glutamate catabolism (24) led us to suppose that unphosphorylated OdhI can function as an inhibitor of ODH.

Purification of a Mixed ODH·PDH Complex—Generally, ODH is a large multienzyme complex consisting of oxoglutarate dehydrogenase (E1o), dihydrolipoamide succinyltransferase (E2o), and dihydrolipoamide dehydrogenase (E3) subunits. The proteins encoded by *sucB* (*cg2421*) and *lpd* (*cg0790*) were annotated as putative E2 and E3 subunits of ODH in *C. glutamicum* (16), and Lpd has been biochemically characterized as dihydrolipoamide dehydrogenase (25). Remarkably, corynebacteria and mycobacteria display two unusual features with respect to ODH. The E1o subunit carries an amino-terminal extension bearing sequence similarity to the catalytic domain of E2 subunits (23) (Fig. 4*B*). Moreover, only a single dihydrolipoamide acyltransferase is present in these bacteria (26), in contrast to most other organisms with distinct E2 subunits for ODH and the related PDH complex. Therefore the subunit composition of ODH remained somewhat puzzling. In *M. tuberculosis*, PDH activity could be reconstituted with recombinant AceE, SucB, and Lpd, but no ODH activity was observed by combining SucA (60% sequence identity to *C. glutamicum* OdhA), SucB, and Lpd (26). Instead, SucA was shown to possess a low 2-oxoglutarate decarboxylase activity (27). However, the inability to detect ODH activity in mycobacterial cell extracts as well as with purified proteins might be due to an unusual low stability of this enzyme complex as reported for *C. glutamicum* (13). This instability was also reflected by the fact that our standard purification protocol for Strep-tagged OdhA was not suitable to enrich the putative E2 and E3 subunits of ODH in significant amounts from strain WT-$odhA_{St}$ (Fig. 4*A*, *lane 3*). Therefore, an altered protocol was developed, which allowed enrichment of ODH activity up to an activity of 2.5 units/mg protein. The proteins copurified with Strep-tagged OdhA included SucB (E2) and Lpd (E3), confirming that these three proteins constitute ODH in *C. glutamicum* (Fig. 4*C*, *lane 1*). Surprisingly, minor amounts of AceE, the E1p subunit of PDH (28), were also copurified, and the eluate showed a PDH activity of 0.3 units/mg protein. Vice versa, purification of Strep-tagged AceE from strain WT-$aceE_{St}$ led to copurification of OdhA, SucB, and Lpd (Fig. 4*C*, *lane 2*), and again, the eluate showed both ODH and PDH activity of 0.7 and 1.9 units/mg, respectively. These findings strongly suggest the existence of mixed complexes composed of OdhA, AceE, SucB, and Lpd possessing both ODH and PDH activity.

ODH Activity Is Inhibited by Unphosphorylated OdhI—To verify the assumed function of OdhI as an inhibitor of ODH activity, we first measured the ODH activity in cell extracts of *C. glutamicum* strain Δ*pknG*Δ*odhI* lacking endogenous PknG and OdhI upon addition of purified, unphosphorylated OdhI. As shown in Fig. 5*A*, this resulted in a concentration-dependent hyperbolic inhibition of ODH activity. Half-maximal inhibition was observed at 4.3 nM OdhI. For a more detailed analysis of the inhibition pattern, ODH activity was measured at oxoglutarate concentrations between 0.08 and 1.5 mM and different fixed OdhI concentrations. Primary plots, *e.g.* according to Lineweaver and Burk, were nonlinear, thereby indicating a slightly positive cooperative binding of oxoglutarate (data not shown), as reported for ODH from other organisms (29). The best linear fits in primary Eadie-Scatchard plots (Fig. 5*B*, $v/[S]^n$ *versus* v) were obtained by using a Hill coefficient n_H of 1.24. In these plots, the activities at different OdhI concentrations gave a series of nearly parallel lines with slopes of $-1/K'_{app}$ and intersection points with the abscissa at $V_{max(app)}$. For noninhibited ODH, a V_{max} value of 94 milliunits/mg and an $[S]_{0.5}$ value of 0.22 mM ($K' = [S]^n_{0.5}$) were determined. Double-reciprocal replots of V_{max} minus $V_{max(app)}$ (ΔV_m) and K'_{app} minus K' ($\Delta K'$) *versus* the inhibitor concentration yielded parabolic curves (Fig. 5*B*, *inset*). From the intersection points of these replots with the ordinate, values for α of 1.63 and for β of 0.024 were calculated (nomenclature according to Ref. 30). The latter value has to be treated with caution because the very low ODH activity at high OdhI concentrations is difficult to measure. From these results it can be concluded that OdhI acts as a partial mixed type, essentially noncompetitive inhibitor with respect to oxoglutarate. Application of a linear equation for hyperbolic tight-binding inhibition (31) yielded a K_i value of 2.4 nM.

By using affinity-purified ODH, it was possible to study the influence of PknG-dependent phosphorylation of OdhI on ODH activity without possible interferences from other protein kinases, phosphatases, and ATPases present in cell extracts. As shown above with cell extract, addition of unphosphorylated OdhI inhibited ODH activity. Upon phosphorylation of OdhI by PknG, no inhibition but even a slight stimulation of

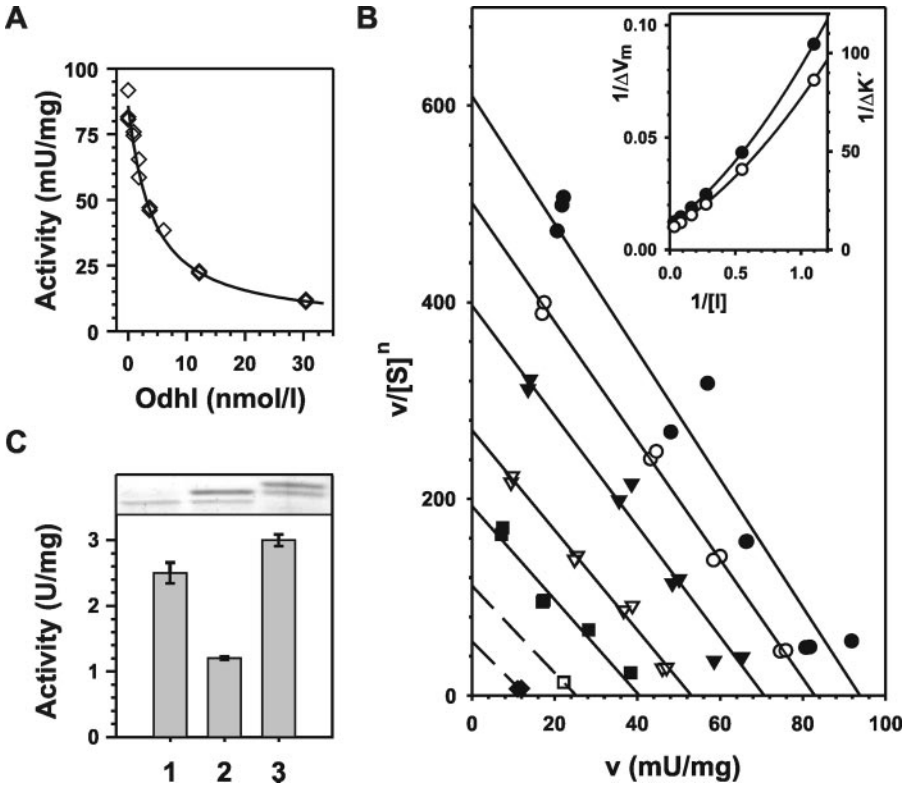

FIGURE 5. **Regulation of ODH activity by the phosphorylation status of OdhI.** *A*, concentration-dependent inhibition of ODH activity in cell extracts of *C. glutamicum* Δ*pknG*Δ*odhI* by addition of purified, unphosphorylated OdhI. The *line* represents the fit of the measured data to the general velocity equation for hyperbolic mixed type inhibition (30). *B*, Eadie-Scatchard plot (using a Hill coefficient $n = 1.24$) of ODH activity in cell extracts at varying oxoglutarate concentrations (0.08, 0.25, 0.5, and 1.5 mM) and different fixed OdhI concentrations: 0 nM (*filled circles*), 0.9 nM (*open circles*), 1.8 nM (*filled triangles*), 3.6 nM (*open triangles*), 6.1 nM (*filled squares*), 12.1 nM (*open squares*), and 30.4 nM (*filled diamonds*). The *solid lines* represent linear fits of the data; the *dashed lines* were calculated as connection to the common intersection point. The *inset* shows a double-reciprocal replot of V_{max} minus $V_{max(app)}$ (ΔV_m; *filled circles*) and K'_{app} minus K' ($\Delta K'$; *open circles*) *versus* the OdhI concentration as calculated from the primary plot. *C*, inhibition of ODH activity by OdhI is abolished by PknG-dependent phosphorylation of OdhI. 2 μg of ODH complex purified from *C. glutamicum* Δ*pknG-odhA*$_{St}$ was incubated for 1 h before activity assays (in triplicate) either without additives (*bar 1*), or with 0.2 μg of OdhI and 2 mM ATP (*bar 2*), or with 0.2 μg of OdhI, 2 mM ATP and 2.2 μg of PknG (*bar 3*). The phosphorylation status of OdhI was verified by SDS-PAGE and mass spectrometric analysis: *bar 1*, native unphosphorylated OdhI; *bar 2*, native and Strep-tagged unphosphorylated OdhI; *bar 3*, native and Strep-tagged phosphorylated OdhI.

ODH activity was observed (Fig. 5*C*), providing further evidence that only the unphosphorylated form of OdhI acts inhibitory. The stimulation can be explained by the assumption that partial inhibition of ODH caused by small amounts of copurified OdhI was abolished after phosphorylation by PknG. The phosphorylation status of OdhI in these experiments was confirmed by SDS-PAGE (Fig. 5*C*, *upper part*) and mass spectrometric analysis. In contrast to ODH, no indications for an influence of OdhI or PknG on PDH activity were found (data not shown).

DISCUSSION

The finding that PknG regulates ODH activity via the phosphorylation status of OdhI represents the first example for participation of serine/threonine protein kinases in the control of this key enzyme of the tricarboxylic acid cycle. In contrast to the well known regulation of mitochondrial PDH activity via phosphorylation of E1p by pyruvate dehydrogenase kinase (32), the mechanism shown here for ODH does not involve direct phosphorylation of ODH subunits by PknG. Rather, it requires the small soluble protein OdhI to mediate signal transduction from PknG, which is at least partially membrane-associated (4, 12),[3] and from membrane integral serine/threonine protein kinases like PknB to cytosolic ODH. Control of the OdhI phosphorylation status by several protein kinases allows integration of different environmental signals to optimally adjust carbon flux distribution at the 2-oxoglutarate node to the prevailing conditions. This mechanism is of particular importance for the biotechnological production of about 1.5 million tons/year of L-glutamate with coryneform bacteria, where attenuation of ODH activity was found to be the key factor in the metabolic network (33). It was shown previously that treatments leading to glutamate excretion, *e.g.* biotin limitation, addition of certain detergents or antibiotics, or cultivation of temperature-sensitive strains at higher temperature, are accompanied by a decrease in ODH activity, but the mechanism remained enigmatic (34, 35). Because of the regulatory function of OdhI and its presumed ability to respond to different stimuli, this protein is the prime candidate for linking the various treatments with the observed metabolic response and therefore a promising target for improving amino acid production.

Considering that the proteins PknG, OdhI (GarA, respectively), and OdhA are highly conserved in corynebacteria and mycobacteria, the signaling cascade involving these proteins might operate also in mycobacteria, an assumption supported by the increased intracellular glutamate/glutamine level measured in an *M. tuberculosis* Δ*pknG* strain (4). PknG is dispensable for growth of *M. bovis* (17) as well as of *C. glutamicum* in nutrient-rich media. In *M. tuberculosis*, the growth defect of the Δ*pknG* mutant was most pronounced in nutrient-depleted media, and an involvement of PknG in sensing nutritional stress was proposed (4). This agrees with our preliminary observation of increased levels of phosphorylated OdhI in carbon-starved *C. glutamicum* (data not shown). Although the metabolism of mycobacteria growing inside macrophages is poorly understood, it has been shown that fatty acids serve as carbon source via the glyoxylate pathway (36), and the tricarboxylic acid cycle is thought to be required to drive ATP synthesis (37). The importance of an intact tricarboxylic acid cycle is further supported by the finding that OdhA is required for growth of *M. tuberculosis* (38). Thus, besides the postulated interference of secreted PknG with host cell signaling pathways (3), delayed virulence and decreased ability to block phagosome-lysosome fusion of mycobacteria lacking PknG might also be explained by a disturbed energy metabolism because of inhibition of ODH.

Acknowledgments—We thank our colleagues C. Trötschel, A. Burkovski, and R. Krämer for help with glutamine uptake measurements; L. Eggeling, B. J. Eikmanns, S. Rospert, and V. F. Wendisch for critical reading of the manuscript; S. Schaffer for contributions in the initial phase of this study, and H. Sahm for continuous support.

[3] A. Niebisch, A. Kabus, C. Schultz, B. Weil, and M. Bott, unpublished results.

REFERENCES

1. Kennelly, P. J. (2002) *FEMS Microbiol. Lett.* **206,** 1–8
2. Av-Gay, Y., and Everett, M. (2000) *Trends Microbiol.* **8,** 238–244
3. Walburger, A., Koul, A., Ferrari, G., Nguyen, L., Prescianotto-Baschong, C., Huygen, K., Klebl, B., Thompson, C., Bacher, G., and Pieters, J. (2004) *Science* **304,** 1800–1804
4. Cowley, S., Ko, M., Pick, N., Chow, R., Downing, K. J., Gordhan, B. G., Betts, J. C., Mizrahi, V., Smith, D. A., Stokes, R. W., and Av-Gay, Y. (2004) *Mol. Microbiol.* **52,** 1691–1702
5. Eggeling, L., and Bott, M. (eds) (2005) *Handbook of Corynebacterium glutamicum*, CRC Press, Inc., Boca Raton, FL
6. Alderwick, L. J., Radmacher, E., Seidel, M., Gande, R., Hitchen, P. G., Morris, H. R., Dell, A., Sahm, H., Eggeling, L., and Besra, G. S. (2005) *J. Biol. Chem.* **280,** 32362–32371
7. Keilhauer, C., Eggeling, L., and Sahm, H. (1993) *J. Bacteriol.* **175,** 5595–5603
8. Niebisch, A., and Bott, M. (2001) *Arch. Microbiol.* **175,** 282–294
9. Wittmann, C., Krömer, J. O., Kiefer, P., Binz, T., and Heinzle, E. (2004) *Anal. Biochem.* **327,** 135–139
10. Krämer, R., Lambert, C., Hoischen, C., and Ebbighausen, H. (1990) *Eur. J. Biochem.* **194,** 929–935
11. Schaffer, S., Weil, B., Nguyen, V. D., Dongmann, G., Günther, K., Nickolaus, M., Hermann, T., and Bott, M. (2001) *Electrophoresis* **22,** 4404–4422
12. Koul, A., Choidas, A., Tyagi, A. K., Drlica, K., Singh, Y., and Ullrich, A. (2001) *Microbiology* **147,** 2307–2314
13. Shiio, I., and Ujigawatakeda, K. (1980) *Agric. Biol. Chem.* **44,** 1897–1904
14. Weinstein, E. A., Yano, T., Li, L. S., Avarbock, D., Avarbock, A., Helm, D., McColm, A. A., Duncan, K., Lonsdale, J. T., and Rubin, H. (2005) *Proc. Natl. Acad. Sci. U. S. A.* **102,** 4548–4553
15. Siewe, R. M., Weil, B., and Krämer, R. (1995) *Arch. Microbiol.* **164,** 98–103
16. Kalinowski, J., Bathe, B., Bartels, D., Bischoff, N., Bott, M., Burkovski, A., Dusch, N., Eggeling, L., Eikmanns, B. J., Gaigalat, L., Goesmann, A., Hartmann, M., Huthmacher, K., Krämer, R., Linke, B., McHardy, A. C., Meyer, F., Möckel, B., Pfefferle, W., Pühler, A., Rey, D. A., Rückert, C., Rupp, O., Sahm, H., Wendisch, V. F., Wiegrabe, I., and Tauch, A. (2003) *J. Biotechnol.* **104,** 5–25
17. Nguyen, L., Walburger, A., Houben, E., Koul, A., Muller, S., Morbitzer, M., Klebl, B., Ferrari, G., and Pieters, J. (2005) *J. Bacteriol.* **187,** 5852–5856
18. Belanger, A. E., and Hatfull, G. F. (1999) *J. Bacteriol.* **181,** 6670–6678
19. Pallen, M., Chuadhuri, R., and Khan, A. (2002) *Trends Microbiol.* **10,** 556–563
20. Villarino, A., Duran, R., Wehenkel, A., Fernandez, P., England, P., Brodin, P., Cole, S. T., Zimny-Arndt, U., Jungblut, P. R., Cervenansky, C., and Alzari, P. M. (2005) *J. Mol. Biol.* **350,** 953–963
21. Molle, V., Kremer, L., Girard-Blanc, C., Besra, G. S., Cozzone, A. J., and Prost, J. F. (2003) *Biochemistry* **42,** 15300–15309
22. Molle, V., Soulat, D., Jault, J. M., Grangeasse, C., Cozzone, A. J., and Prost, J. F. (2004) *FEMS Microbiol. Lett.* **234,** 215–223
23. Usuda, Y., Tujimoto, N., Abe, C., Asakura, Y., Kimura, E., Kawahara, Y., Kurahashi, O., and Matsui, H. (1996) *Microbiology* **142,** 3347–3354
24. Shiio, I., Ozaki, H., and Mori, M. (1982) *Agric. Biol. Chem.* **46,** 493–500
25. Schwinde, J. W., Hertz, P. F., Sahm, H., Eikmanns, B. J., and Guyonvarch, A. (2001) *Microbiology* **147,** 2223–2231
26. Tian, J., Bryk, R., Shi, S. P., Erdjument-Bromage, H., Tempst, P., and Nathan, C. (2005) *Mol. Microbiol.* **57,** 859–868
27. Tian, J., Bryk, R., Itoh, M., Suematsu, M., and Nathan, C. (2005) *Proc. Natl. Acad. Sci. U. S. A.* **102,** 10670–10675
28. Schreiner, M. E., Fiur, D., Holatko, J., Patek, M., and Eikmanns, B. (2005) *J. Bacteriol.* **187,** 6005–6018
29. Kornfeld, S., Benziman, M., and Milner, Y. (1977) *J. Biol. Chem.* **252,** 2940–2947
30. Segel, I. H. (1975) *Enzyme Kinetics*, pp. 161–226, John Wiley & Sons, Inc., New York
31. Szedlacsek, S. E., Ostafe, V., Serban, M., and Vlad, M. O. (1988) *Biochem. J.* **254,** 311–312
32. Linn, T. C., Pettit, F. H., and Reed, L. J. (1969) *Proc. Natl. Acad. Sci. U. S. A.* **62,** 234–241
33. Shirai, T., Nakato, A., Izutani, N., Nagahisa, K., Shioya, S., Kimura, E., Kawarabayasi, Y., Yamagishi, A., Gojobori, T., and Shimizu, H. (2005) *Metab. Eng.* **7,** 59–69
34. Uy, D., Delaunay, S., Goergen, J. L., and Engasser, J. M. (2005) *Bioproc. Biosyst. Eng.* **27,** 153–162
35. Kawahara, Y., Takahashi-Fuke, K., Shimizu, E., Nakamatsu, T., and Nakamori, S. (1997) *Biosci. Biotechnol. Biochem.* **61,** 1109–1112
36. Munoz-Elias, E. J., and McKinney, J. D. (2005) *Nat. Med.* **11,** 638–644
37. Boshoff, H. I. M., and Barry, C. E. (2005) *Nat. Rev. Microbiol.* **3,** 70–80
38. Sassetti, C. M., Boyd, D. H., and Rubin, E. J. (2003) *Mol. Microbiol.* **48,** 77–84
39. Kinoshita, S., Udaka, S., and Shimono, M. (1957) *J. Gen. Appl. Microbiol.* **3,** 193–205
40. Eikmanns, B. J., Kleinertz, E., Liebl, W., and Sahm, H. (1991) *Gene* (*Amst.*) **102,** 93–98
41. Cremer, J., Eggeling, L., and Sahm, H. (1990) *Mol. Gen. Genet.* **220,** 478–480
42. Schäfer, A., Tauch, A., Jäger, W., Kalinowski, J., Thierbach, G., and Pühler, A. (1994) *Gene* (*Amst.*) **145,** 69–73